

The Role of Thermal Conduction in Accretion Disks with Outflows

Jamshid Ghanbari^{1,2}, Arezoo Tajmohammadi¹

¹ Department of Physics, School of Sciences, University of Mashhad, (FUM) 91775-1436, Iran;
email: ghanbari@um.ac.ir

² Department of Physics, Khayyam Institute of Higher Education, Mashhad, Iran

Abstract. In this work we solve the set of hydrodynamical equations for accretion disks in the spherical coordinates (r, θ, ϕ) to obtain the explicit structure along θ direction. We study a two-dimensional advective accretion disc in the presence of thermal conduction. We find self-similar solutions for an axisymmetric, rotating, steady, viscous-resistive disk. We show that the global structure of an advection-dominated accretion flow (ADAFs) is sensitive to viscosity, advection, wind and thermal conduction parameters. We discuss how the radial flows, meridional velocity, rotation velocity, sound speed and density of accretion flows may vary with the advection, thermal conduction and wind parameters. We will find that the radial velocity in nearby the equator, angular velocity and sound speed decrease by increasing the thermal conduction parameter and meridional velocity increases by increasing it.

Keywords: accretion disk, wind, thermal conduction

1 Introduction

Accretion on compact objects are the most energetic process in the universe, powering x-ray binaries and nuclei of galaxies [1, 2]. It is believed that many astrophysical objects are powered by mass accretion on to black holes. The standard geometrically thin, optically thick accretion disk model can successfully explain most of the observational features in active galactic nuclei (AGN) and X-ray binaries [3]. The thin accretion disk model describes flows in which the viscous heating of the gas radiates out the system immediately after generation [3]. However, another kind of accretion has been studied during recent years where radiative energy losses are small so that most of the energy is advected within the gas.

These Advection Dominated Accretion Flows (ADAF) occur in two regimes depending on the mass accretion rate and the optical depth. At very high mass accretion rate, the optical depth becomes very high and the radiation can be trapped in the gas. This type of accretion which is known under the name 'slim accretion disk' has been studied in detail by Abramowicz et al (1988)[4]. But when the accretion rate is very small and the optical depth is very low, we may have another type of accretion [5, 6, 7].

These types of solutions have been used to interpret the spectra of X-ray binary black holes in their quiescent or low/hard state as an alternative to the Shapiro, Lightman and Eardly (1976, SLE)[8] solutions. Since ADAFs have large radial velocities, and also in falling matter carries thermal energy to the black hole, the energy transported by advection can stabilize the thermal instability by removing their steep temperature gradients: thus the ADAF models have been widely used to explain the observations of low luminosity observed in Sgr A* [9, 10]. However, Numerical simulations of radiation inefficient accretion

flows revealed that the low-viscosity flows are convectively unstable, and therefore convection strongly influences the global structure of accretion flows [11]. Thus another type of accretion flow was proposed, in which the convection plays the dominated role in transporting the energy- angular momentum and locally released viscose energy within the disk.

The observations of black holes confirm the existence of hot accretion flows that contrasted with classical cold and thin accretion discs models [3]. Hot accretion flows can be seen in super massive black holes of galactic nuclei and during quiescent of accretion on to stellar-mass black holes in X-ray transients and also on the hard state of XRBs [12, 13, 14]. Chandra's observations provide constraints on the density and temperature of gas at or near the Bondi capture radius in Sgr A* and several nearby galactic nuclei [15, 16, 17, 18]. Tanaka & Menou (2006) [19] have shown through their calculations that the accretion disks in such systems will operate under weakly collisional conditions. Thermal conduction therefore has an important role in energy transport along the disks. The aim of this work is to consider the effect of thermal conduction, which has been largely neglected before as an energy transport mechanism, on the 2D structure of ADAFs. It could affect the global properties of hot accretion flows substantially. A few authors have considered the role of turbulent heat transport in ADAF discs [20, 21, 19]. Since thermal conduction acts that oppose the formation of temperature gradient that causes it, one might expect that the temperature and density profile for accretion flows in which thermal conduction plays a significant role; are modified to appear different, compared with those flows form which thermal conduction is less effective [22].

The Weak-collisions nature of hot accretion flows has been addressed previously [23] studied the effect of electron thermal conduction on the properties of hot accretion flows under the assumption of spherical symmetry. In another interesting analysis, Tanaka & Menou (2006)[19], studied the effect of saturated thermal conduction on optically thin ADAFs using an extension of self-similar solution of Narayan & Yi (1994) [5]. In their solutions, the thermal conduction is provided an extra degree of freedom which affects the global dynamical behaviors of the accretion flow. Also Narayan & Yi (1995)[24], used self-similar assumptions in the radial direction and solved the structure along the θ direction in spherical coordinates (r, θ, φ) . Abbassi, Ghanbari & Najjar (2008) [25] have presented a set of self-similar solutions for ADAFs with a toroidal magnetic field in which the saturated thermal conduction has a great role in the energy transport in the radial direction.

Also now several self-similar solutions of ADAFs with outflow have been presented in different papers [22, 26, 27, 28, 29, 30]. The equations that describe the hydrodynamical processes are the Navier-Stokes equations, which are quite difficult to solve, in the case of accretion disks which involve viscosity and radiation. Therefore in most works, some kind of simplifications, such as one-zone or polytropic distribution and hydrostatic equilibrium, are usually applied in the vertical direction, and the vertical variation, z , of the velocity field is usually neglected. In this way the equations are changed to a set of ordinary differential equations(ODEs) in the radial direction, which can be solved numerically. However, by taking these assumptions, one cannot get a clear picture of the vertical structure of accretion flows; the velocity is always radially inward and no mass will cross the disk surface, displaying no outflow structure. Among the exceptions is a work done by Narayan & Yi in 1995 (hereafter NY95)[24], which used self-similar assumptions in the radial direction and solved the structure along the θ direction in spherical coordinates (r, θ, φ) . However in their work they assumed $v_\theta = 0$ and thus cannot get proper velocity field and their solutions compose of only pure inflow. They argued that the Bernoulli parameter is positive in their solutions so that a bipolar outflow is expected to develop near the vertical axis. Blandford & Begelman (1999, hereafter BB99)[31] relaxed the mass conservation assumption and assumed that the mass inflow rate varies with radius, and obtained solutions with outflow called adiabatic

inflow-outflow solutions (ADIOs). Their solutions are one-dimensional self-similar solutions that are height-averaged and they also applied the Bernoulli parameter to argue the presence of outflow. However, Abramowicz et al. (2000)[32] pointed out that positive Bernoulli function is not sufficient for outflow (also see the simulation works done by Stone et al. 1999 and Yuan & Bu 2010)[33, 34]. Blandford & Begelman (2004)[35] furthered the work and presented some self-similar two-dimensional solutions of radiatively inefficient accretion flows with outflow. They assumed hydrostatic equilibrium in the vertical direction and that convection dominates the heat transport, which may only be applicable in certain cases. Xu & Chen (1997, hereafter XC97) [36] relaxed $v_\theta = 0$ and obtained two types of solutions with outflow: accretion and ejection solutions. However their solutions require the net accretion rate to be 0, which is not realistic. Xue & Wang (2005, hereafter XW05)[37] followed NY95 and solved the disk structure along the θ direction considering . Their solutions display a field of inflow near the equatorial plane with wind blowing out of the upper boundary.

Now we follow the work done by NY95 and XW05 by using self-similar assumptions in radial direction. In order to solve the ODEs along θ direction in spherical coordinates (r, θ, φ) , we would consider the thermal conduction as well. We try to find the flow structure dependence on some parameters in order to understand the inflow/outflow mechanism more physically.

2 The Basic Equations

Three conservation equations: mass, momentum, and energy conservation equations. They can be respectively written as

$$\nabla \cdot (\rho \mathbf{u}) = 0 \quad (1)$$

$$\rho \mathbf{u} \cdot \nabla \mathbf{u} = -\nabla P - \rho \nabla \varphi + \nabla \cdot \mathbf{T} \quad (2)$$

$$\rho(\mathbf{u} \cdot \nabla e - \frac{P}{\rho^2} \mathbf{u} \cdot \nabla \rho) = f \nabla \mathbf{u} : \mathbf{T} - \nabla \cdot \mathbf{F}_s, \quad (3)$$

where $\rho, \mathbf{u}, P, \varphi, \mathbf{T}, e$ and f are mass density, velocity vector, gas pressure, gravitational potential, tensor of viscous stress, internal energy of gas, and advective fraction of viscous dissipation. Also $F_s = 5\phi_s \rho c_s^2$ is the saturated conduction flux [38]. Dimensionless coefficient ϕ_s is less than unity. Tanaka & Menou (2006) have shown that for very small ϕ_s their solutions coincide with the standard ADAF solutions.

We employ the parameter $f = 1 - (\frac{Q_-}{Q_+})$ to measure the degree to which accretion flow is advection-dominated. When $f \approx 1$ the radiation can be neglected and the accretion flow is advection-dominated [39]. We assume that the problem is axi-symmetric and in steady state, $(\partial/\partial\varphi = \partial/\partial t = 0)$. Now we formulate the basic equations (1)-(3) in spherical polar coordinates as follows:

$$\frac{1}{r^2} \frac{\partial}{\partial r} (r^2 \rho v_r) + \frac{1}{r \sin \theta} \frac{\partial}{\partial \theta} (\sin \theta \rho v_\theta) = 0 \quad (4)$$

The three components of the momentum equation are as follows :

$$\begin{aligned} \rho [V_r \frac{\partial V_r}{\partial r} + \frac{V_\theta}{r} (\frac{\partial V_r}{\partial \theta} - V_\theta) - \frac{V_\phi^2}{r}] &= -\frac{GM\rho}{r^2} - \frac{\partial P}{\partial r} + \\ 2[\frac{1}{r^2 \sin \theta} \frac{\partial}{\partial r} (r^2 \sin \theta T_{11}) + \frac{\partial}{\partial \theta} (r \sin \theta T_{12}) - \frac{T_{22} + T_{33}}{r}] & \quad (5) \\ \rho [V_r \frac{\partial V_\theta}{\partial r} + \frac{V_\theta}{r} (\frac{\partial V_\theta}{\partial \theta} + V_r) - \frac{V_\phi^2}{r} \cot \theta] &= -\frac{1}{r} \frac{\partial p}{\partial r} + 2[\frac{1}{r \sin \theta} \end{aligned}$$

$$\frac{\partial}{\partial r}(r \sin \theta T_{21}) + \frac{\partial}{\partial \theta}(\sin \theta T_{22}) - \frac{T_{33} \cot \theta - 2T_{21}}{r} \quad (6)$$

$$\rho[V_r \frac{\partial V_\phi}{\partial r} + \frac{V_\theta}{r}(\frac{\partial V_\phi}{\partial \theta}) + \frac{V_\phi}{r}(V_r + V_\theta \cot \theta)] = \frac{2}{r}(\frac{\partial}{\partial r}(r T_{31}) + \frac{\partial T_{32}}{\partial \theta}) + \frac{4}{r}(T_{31} + T_{32} \cot \theta) \quad (7)$$

where T_{ij} is the component of stress tensor \mathbf{T} . (see the detailed form of viscous stress tensor in Appendix A). The energy conservation is

$$\begin{aligned} \rho[(V_r \frac{\partial e}{\partial r} + \frac{V_\theta}{r} \frac{\partial e}{\partial \theta}) - \frac{p}{\rho^2}(V_r \frac{\partial \rho}{\partial \theta} + V_\theta \frac{\partial \rho}{\partial r})] &= 2f[\frac{\partial V_r}{\partial r} T_{11} + \frac{\partial V_\theta}{\partial r} T_{21} + \frac{\partial V_\phi}{\partial r} T_{31} + \\ \frac{1}{r}(\frac{\partial V_r}{\partial \theta} - V_\theta) T_{12} + \frac{1}{r}(\frac{\partial V_\theta}{\partial \theta} + V_r) T_{22} + \frac{1}{r} \frac{\partial V_\phi}{\partial \theta} T_{32} - \frac{V_\phi}{r}(T_{13} + T_{23} \cot \theta) + \\ \frac{T_{33}}{r}(V_r + V_\theta \cot \theta)] - \frac{1}{r^2} \frac{\partial}{\partial r}(5\phi_s r_2 p^{3/2} \rho^{-1/2}) - \frac{1}{r \sin \theta} \frac{\partial}{\partial \theta}(5\phi_s \sin \theta p^{3/2} \rho^{-1/2}), \end{aligned} \quad (8)$$

The solutions of these equations ,(4)-(8), are strongly dependent on viscosity, the degree of advection, wind and the role of thermal conduction for the discs. For the set of equations, we use the following standard assumptions: The kinematics viscosity coefficient, $\nu = \mu/\rho$, is generally parameterized using the α -prescription [3].

$$\nu = \alpha c_s H, \quad (9)$$

where $H = c_s/\Omega_k$ is known as the vertical scale height, $c_s = \sqrt{P/\rho}$ is the isothermal sound speed and the dimensionless coefficient α is assumed to be independent of r . To determine the thermodynamical properties of the flow in the energy equation, we require a constitutive relation as a function of two state variables. Therefore we choose an equation for the internal energy of $e = \frac{c_s^2}{\gamma-1}$ where γ is the ratio of specific heats and c_s is isothermal sound speed.

3 Self-Similar Solutions

We adopt the self-similar assumptions in the radial direction; therefore we seek solutions of the forms

$$\rho = \rho(\theta) r^{-n} \quad (10)$$

$$V_r = V_r(\theta) V_k \quad (11)$$

$$V_\theta = V_\theta(\theta) V_k \quad (12)$$

$$V_\phi = V_\phi(\theta) V_k \quad (13)$$

$$c_s = c_s(\theta) V_k \quad (14)$$

where

$$V_k = \sqrt{\frac{GM}{r}} \quad (15)$$

This set of self-similar solutions, instead of equation(13), are similar to that of NY95 and Tanaka & Menou (2006) [19]. Equation (13) is similar to that of XW05 [37] and Jiao & Yuan (2012)[30]. The results are unaffected by this difference. In NY95, Narayan and Yi set $n=3/2$, which implies $V_\theta = 0$, according to the continuity equation, thus they intrinsically set

no outflow for the accretion disk. Here we relax this parameter n , following BB99 and XW05, to allow outflows from the disk. If we substitute equations (10)-(14) into equations (4)-(8), the r components can be eliminated, leaving only the dimensionless functions $\rho(\theta)$, $V_r(\theta)$, $V_\theta(\theta)$, $V_\phi(\theta)$, $c_s(\theta)$, the variable θ and some constants which are set as input parameters (α , n , f and ϕ_s). The equations are as follows:

$$2V_\theta \frac{d\rho}{d\theta} + \rho \left\{ (3 - 2n)V_r + 2(\cos \theta V_\theta + \frac{dV_\theta}{d\theta}) \right\} = 0 \quad (16)$$

$$3\alpha \frac{d(\rho c_s^2)}{d\theta} (3V_\theta - 2\frac{dV_r}{d\theta}) - \rho \{ 3(V_r^2 + 2V_\theta^2 + 2V_\phi^2 - 2V_\theta \frac{dV_r}{d\theta} - 2) + c_s^2 [\alpha(4n - 17)(\cot \theta + \frac{dV_\theta}{d\theta}) + 6\alpha(\cot \theta + \frac{d^2 V_r}{d\theta^2}) + 12\alpha(n - 2)V_r + (6 + 6n)] \} = 0, \quad (17)$$

$$\frac{d}{d\theta} [2\rho c_s^2 (3 - 3\alpha V_r + 2\alpha \cot \theta V_\theta - 4\alpha \frac{dV_\theta}{d\theta})] + \rho [3V_\theta (V_r + 2\frac{dV_\theta}{d\theta}) - 6 \cot \theta V_\phi^2] + \alpha \rho c_s^2 [6(n - 2)\frac{dV_r}{d\theta} + (6 - 9n)V_\theta - 12\frac{d}{d\theta}(\cot \theta V_\theta)] = 0, \quad (18)$$

$$\frac{d}{d\theta} [2\alpha \rho c_s^2 (\cot \theta V_\phi - \frac{dV_\phi}{d\theta})] + \rho [V_\phi (V_r + 2 \cot \theta V_\theta) + 2V_\theta \frac{dV_\phi}{d\theta}] + \alpha \rho c_s^2 [(6 - 3n + 4 \cot^2 \theta)V_\phi - 4 \cot \theta \frac{dV_\phi}{d\theta}] = 0, \quad (19)$$

$$\begin{aligned} & \frac{V_r}{\gamma - 1} - \frac{2V_\theta c_s}{(\gamma - 1)c_s^2} \frac{dc_s}{d\theta} - nV_r + V_\theta \frac{d\rho}{d\theta} + 3f\alpha V_r^2 + 2f\alpha V_r \frac{dV_\theta}{d\theta} + 2f\alpha V_r V_\theta \cot \theta \\ & - 3\alpha V_\theta \frac{dV_r}{d\theta} + \frac{9}{4}f\alpha V_\theta^2 + \frac{4}{3}f\alpha V_\theta^2 \cot^2 \theta + \frac{9}{4}f\alpha V_\phi^2 + f\alpha V_\phi^2 \cot^2 \theta + f\alpha (\frac{dV_r}{d\theta})^2 + \\ & \frac{4}{3}f (\frac{dV_\theta}{d\theta})^2 - \frac{4}{3}f\alpha V_\theta \frac{dV_\theta}{d\theta} \cot \theta + f\alpha (\frac{dV_\phi}{d\theta})^2 - 2f\alpha \cot \theta V_\phi \frac{dV_\phi}{d\theta} + 5(n - \frac{1}{2})\phi_s c_s - \\ & 5\phi_s \cot \theta - \frac{5\phi_s}{\rho} \frac{d\rho}{d\theta} = 0 \end{aligned} \quad (20)$$

This set of ODEs can be numerically solved with proper boundary conditions. We assume the structure of the disk is symmetrical to the equatorial plane, and thus we have

$$\theta = 90^\circ : V_\theta = \frac{d\rho}{d\theta} = \frac{dc_s}{d\theta} = \frac{dV_r}{d\theta} = \frac{dV_\phi}{d\theta} = 0 \quad (21)$$

in which only four conditions are independent. For the last boundary condition we set $\rho(90^\circ) = 1$, which can be normalized by a scale factor if the effective accretion rate at a certain radius is set [24, 37], etc. We obtained numerical solutions of equations (16)-(20) with different sets of input parameters (α , f , n , ϕ_s , γ). Some typical solutions are shown in Figures (1)-(5). The calculations start from the equatorial plane ($\theta = 90^\circ$) towards the vertical axis ($\theta = 0^\circ$). Since we can't describe the flow near the vertical axis with a simple self-similar solution in the radial direction, we can describe the upper boundary (minimum θ) that we reach in our calculations as θ_b . Then the effective accretion rate \dot{M}_{eff} across sphere at radius r within the $90^\circ \geq \theta \geq \theta_b$ is.

$$\dot{M}_{eff} = 2 \int_{\theta_b}^{90^\circ} \rho V_r \cdot 2\pi r \sin \theta r \cdot (\pi/180^\circ) d\theta = 4\pi \sqrt{GM} r^{\frac{3}{2}-n}$$

$$\int_{\theta_b}^{90^\circ} \rho(\theta) V_r(\theta) \sin \theta \cdot (\pi/180^\circ) d\theta, \quad (22)$$

which is a function of r unless $n = 3/2$. In equation (22) negative values of \dot{M}_{eff} represent inflow while positive values represent outflow. If we describe the accretion rate in the region between the vertical axis and the inclination angle θ_b as \dot{M}_{axis} , then according to the steady nature of the flow, we have

$$\dot{M}_{eff} + \dot{M}_{axis} = \dot{M} \quad (23)$$

in which \dot{M} represents the total accretion rate across any sphere at a reasonable radius centered by the central accretor and should be constant for a steady accretion flow. If the solution doesn't end at an upper boundary, and instead can describe the entire flow structure in the whole space, then $\theta_b = 0$ and $\dot{M}_{eff} = \dot{M}$, which should be a constant. According to equation (22), this can only happen in the following two cases: (1) $n = 3/2$ which enforces \dot{M}_{eff} not to change with radius r , (2) when $n \neq 3/2$, the integration term in equation (22) must be 0, in which case $\dot{M}_{eff} = 0$. The first case was discussed in NY95. Because $n = 3/2$, $r^2 \rho V_r$ is independent of r , and the continuity equation (1) shows that $V_\theta = 0$, resulting in a solution in which the flow is always radial (wind rotation). The second case was discussed in XC97, and the fact that $\dot{M} = 0$ requires that the outflow rate exactly equals the inflow rate at any radius. However this is unrealistic for an accretion flow, which is also discussed in XW05. The reason is that, when material is accreted in the form of an accretion flow, gravitational energy is released and part of it, is changed to internal energy via viscous friction. The restriction that outflow rate equals inflow rate requires that the internal energy released from gravitational energy should be fully returned to gravitational energy, which violates the second law of thermodynamics.

4 Numerical Results

There are six parameters, $n, \alpha, \theta_0, r, \phi_s$ and f in our model. The exponent of density profile, n , is an index of inflow/outflow (when n increases, the inflow increases and the outflow decreases), but there is always more inflow material than outflow material, and it has $1/2 \leq n \leq 3/2$. The parameter α is an index of viscosity, and $0 < \alpha < 1$. In this paper we present three types of solutions with different inflow/outflow indices $n = (1.25, 1, 0.75)$.

Figure 1 shows the variations of various dynamical quantities in terms of polar angle θ for fixed values of viscosity, thermal conduction and wind parameters with a sequence of decreasing advection parameter f . We can see by decreasing advection parameter f , V_ϕ and c_s increase. Also V_r in about the equatorial plane decreases with increasing advection parameter. While V_θ decreases by decreasing f .

Figure 2 displays the behaviour of $V_r(\theta)$, $V_\theta(\theta)$, $V_\phi(\theta)$ and c_s for different values of the viscosity parameter. We find that the value of the viscous parameter, α , quantitatively affects the dynamical variable of the accretion flow. By increasing viscous parameter α , the quantities $V_\theta(\theta)$, c_s and also V_r in nearby the equatorial plane increase, while $V_\phi(\theta)$ decreases by increasing α . In this case, increasing the viscosity parameter corresponds to increase heating mechanism, so in fixed advection regime, there is more energy to advect into the central star.

Figure 3 shows by decreasing, n , the velocity quantities $V_\theta(\theta)$, $V_\phi(\theta)$ and sound speed c_s decrease. While V_r in the rang $(45^\circ - 65^\circ)$ increases by decreasing n . But it decreases among 65° and 90° by decreasing n . We can see that ADAFs with winds rotate more quickly than

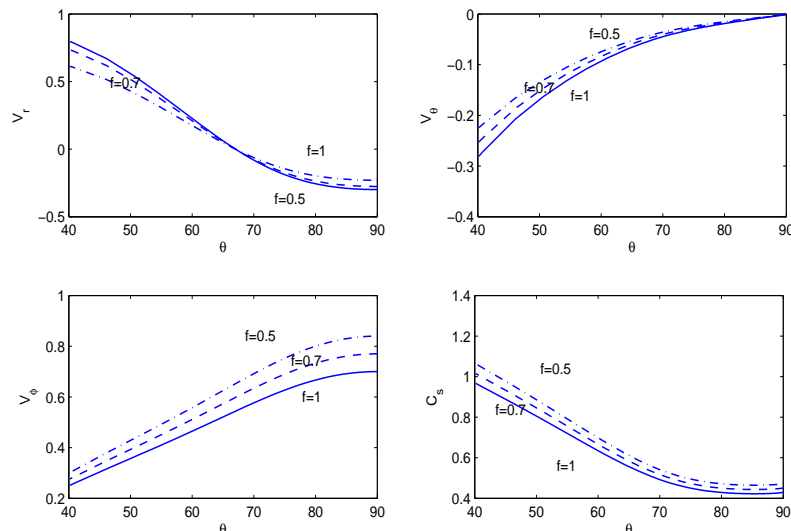


Figure 1: Numerical results for $n = 1.25$, $\alpha = 0.3$, $\phi_s = 0.0001$ and $\gamma = 1.4$.

those without winds. Also, the viscous dissipation is expected to be larger in the presence of winds and outflows.

The panels in Figure 4 show how $V_r(\theta)$, $V_\theta(\theta)$ and $V_\phi(\theta)$ change with θ and ϕ_s . We consider the disk to be radiation dominated with $n = 1.25$, $\alpha = 0.3$, $f = 1$ and $\gamma = 1.4$, which is the widely used values. We can see radial velocity in around the equator, angular velocity and sound speed decrease by increasing the thermal conduction parameter and meridional velocity increases by increasing ϕ_s .

Actually, outflows play as a cooling agent and thermal conduction provides extra heating and there is a competition between these physical factors. While the effects of winds and thermal conduction on $V_r(\theta)$, $V_\phi(\theta)$ and the sound speed is similar, their effect on $V_\theta(\theta)$ oppose each other.

In Figure 5 we can see by increasing γ , radial velocity in nearby the equator decreases and meridional velocity, rotation velocity and sound speed increase by increasing γ . We can see that the gas adiabatic index contributes with thermal conduction to reduce advection transport of energy.

5 Conclusions

We follow the work done by NY95 and XW05 by using self similar assumptions in radial direction. In order to solve the ODEs along θ direction in spherical coordinates (r, θ, ϕ) , we considered the thermal conduction as well. Our conclusions are listed as follows:

(1) In ADAFs with wind when decrease, n , increases outflow and radial velocity in nearby the equator, sound speed, meridional velocity, rotation velocity and density decrease. We can see that ADAFs with winds rotate more quickly than those without winds. Also, the viscous dissipation is expected to be larger in the presence of winds and outflows.

(2) The radial velocity in the range $65^\circ - 90^\circ$, angular velocity and sound speed decrease by increasing the thermal conduction parameter and meridional velocity increases by

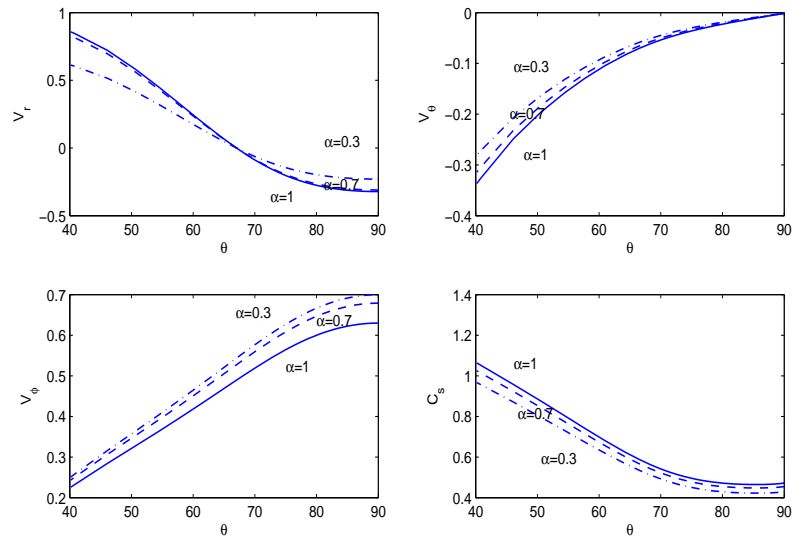


Figure 2: Numerical results for $n = 1.25$, $\phi_s = 0.0001$, $f = 1$ and $\gamma = 1.4$.

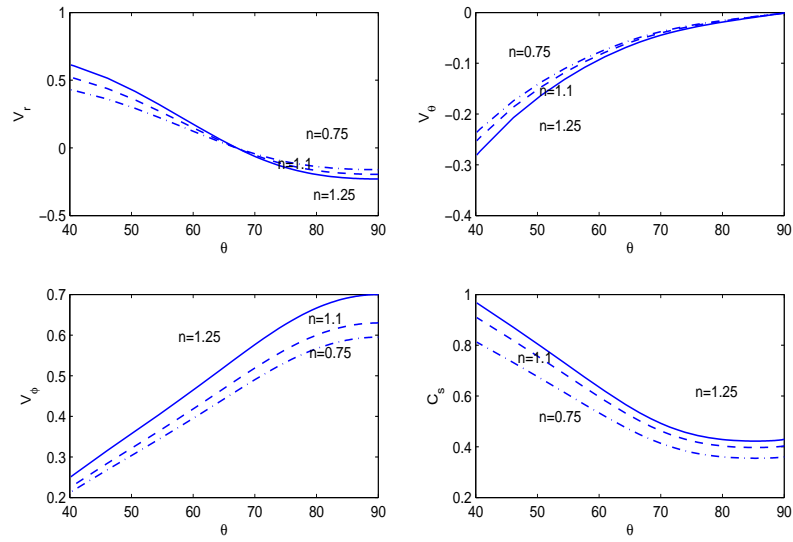


Figure 3: Numerical results for $\alpha = 0.3$, $\phi_s = 0.0001$, $f = 1$ and $\gamma = 1.4$.

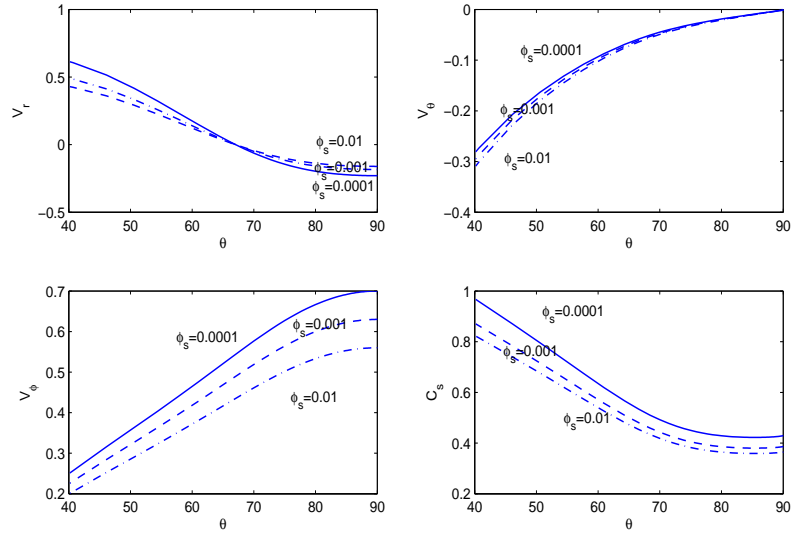


Figure 4: Numerical results for $n = 1.25$, $\alpha = 0.3$, $f = 1$ and $\gamma = 1.4$.

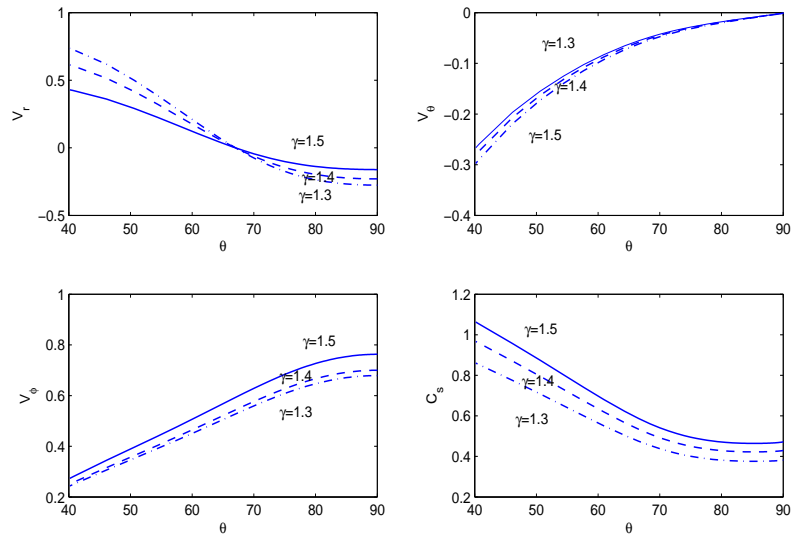


Figure 5: Numerical results for $n = 1.25$, $\alpha = 0.3$, $\phi_s = 0.0001$ and $f = 1$.

increasing ϕ_s . Actually, outflow plays as a cooling agent and thermal conduction provides extra heating and there is a competition between these physical factors.

(3) By decreasing advection parameter, V_r in about the equator, V_ϕ and c_s increase. While V_θ decreases by decreasing f .

(4) We can see by increasing viscous parameter, V_r in nearby the equator, V_θ and c_s increase while V_ϕ decreases by increasing α . In this case, by increasing the viscosity parameter, α , corresponding to increase heating mechanism, so in fixed advection regime, there is more energy to advect into the central star.

(5) By increasing γ , radial velocity in around the equatorial plane decreases while sound speed, meridional velocity and rotation velocity increase by increasing γ . We can see that the gas adiabatic index contributes with thermal conduction to reduce advection transport of energy.

APPENDIX A

The components of viscous stress tensor are

$$\begin{aligned}
 T_{11} &= \mu \left[\frac{\partial V_r}{\partial r} - \frac{1}{3} \left[\frac{1}{r^2} \frac{\partial}{\partial r} (r^2 V_r) + \frac{1}{r \sin \theta} (\sin \theta V_\theta) \right] \right] \\
 T_{12} &= \mu \left[\frac{1}{2} \left[\frac{1}{r} \frac{\partial V_r}{\partial \theta} + r \frac{\partial}{\partial r} \left(\frac{V_\theta}{r} \right) \right] \right] \\
 T_{13} &= \mu \left[\frac{r}{2} \frac{\partial}{\partial r} \left(\frac{V_\theta}{r} \right) \right] \\
 T_{21} &= \mu \left[\frac{1}{2} \left[\frac{1}{r} \frac{\partial V_r}{\partial \theta} + r \frac{\partial}{\partial r} \left(\frac{V_\theta}{r} \right) \right] \right] \\
 T_{22} &= \left[\mu \frac{1}{r} \frac{\partial V_\theta}{\partial \theta} + \frac{V_r}{r} - \frac{1}{3} \left[\frac{1}{r^2} \frac{\partial}{\partial r} (r^2 V_r) + \frac{1}{r \sin \theta} \frac{\partial}{\partial \theta} (\sin \theta) \right] \right] \\
 T_{23} &= \mu \left[\frac{\sin \theta}{2r} \frac{\partial}{\partial \theta} \left(\frac{V_\phi}{\sin \theta V_\theta} \right) \right] \\
 T_{31} &= \mu \left[\frac{r}{2} \frac{\partial}{\partial r} \left(\frac{V_\phi}{r} \right) \right] \\
 T_{32} &= \mu \left[\frac{\sin \theta}{2r} \frac{\partial}{\partial \theta} F \left(\frac{V_\phi}{\sin \theta} \right) \right] \\
 T_{33} &= \mu \left[\frac{V}{r} + \frac{V_\theta}{r} \cot \theta - \frac{1}{3} \left[\frac{1}{r^2} \frac{\partial}{\partial r} (r^2 V_r) + \frac{1}{r \sin \theta} \frac{\partial}{\partial \theta} (\sin \theta V_\theta) \right] \right]
 \end{aligned}$$

References

- [1] Frank J., King A., Raine D., 2002, *Accretion Power in Astrophysics*. Cambridge Univ. Press, Cambridge
- [2] Kato S., Fukue J., Mineshige S., 2008, *Black-Hole Accretion Disks: Towards a New Paradigm*. Kyoto Univ.press, Kyoto
- [3] Shakura, N. I., Sunyaev R. A., 1973, *A&A*, 24 ,337
- [4] Abramowicz M. A., Czerny B., Lasota J. P., Szuszkiewicz E., 1988, *ApJ*, 332, 646
- [5] Narayan R., Yi I., 1994, *ApJ*, 428, L13

- [6] Abramowicz M. A., Chen X., Kato S., Lasota J. P., Regev O., 1995, *ApJ*, 438, L37
- [7] Chen X., 1995, *MNRAS*, 275, 641
- [8] Shapiro S. L., Lightman A. P., Eardley D. M., 1976, *ApJ*, 204, 187
- [9] Narayan R., Maclintock J. E., Yi I., 1996, *ApJ*, 457, 821
- [10] Hameury J. M., Lasota J. P., Maclintock J. E., Narayan R., 1997, *ApJ*, 489, 234
- [11] Igumenshchev I. V., Abramowicz, M. A. 2000, *ApJS*, 130, 463
- [12] Lasota J. P., Abramowicz M. A., Chen X., Krolik J., Narayan R., Yi., 1996, *ApJ*, 462, 192
- [13] Yuan F., 2007, in the Central Engine of Active Galactic Nuclei, ASP Conference Series, eds. L. C. Ho and J. M. Wang, Vol. 373, p.95
- [14] Narayan R., McClintock J. E., 2008, *NewAR*, 51, 733
- [15] Loewenstein M., Mushotzky R. F., Angelini L., Arnaud K. A., Quataert, E., 2001, *ApJ*, 555, L21
- [16] Bagnoff F. K., et al., 2003, *ApJ*, 591, 891
- [17] Di Matteo T., Allen S. W., Fabian A. C., Wilson A. S., Young, A. J., 2003, *ApJ*, 582, 133
- [18] Ho L. C., Terashima Y., Ulvestad J. S., 2003, *ApJ*, 589, 783
- [19] Tanaka T., Menou., 2006, *ApJ*, 649, 345
- [20] Honma F., *PASJ*, 1996, 48, 77
- [21] Manmoto T., Kato S., Nakamura K., Narayan R., 2000, *ApJ*, 529, 127
- [22] Shadmehri M., 2008, *Ap&SS*, 317, 201
- [23] Mahadevan R., Quataert E., 1997, *ApJ*, 490, 605
- [24] Narayan R., Yi I., 1995, *ApJ*, 444, 231
- [25] Abbassi S., Ghanbari G., Najjar S., 2008, *MNRAS*, 388, 663
- [26] Fukue J., 1989, *PASJ*, 41, 123
- [27] Takahara F., Rosner R., Kusnose M., 1989, *ApJ*, 346, 122
- [28] Abbassi S., Ghanbari G., Ghasemnezhad M., 2010, *MNRAS*, 409, 1113
- [29] Xie F., Yuan F., 2008, *ApJ*, 681, 499
- [30] Jiao C., Wu X., 2011, *ApJ*, 733, 112
- [31] Blandford R. D., Begelman M. C., 1999, *MNRAS*, 303, L1
- [32] Abramowicz M. A., Lasota J. P., Igumenshchev I. V., 2000, *MNRAS*, 314, 775
- [33] Stone J. M., Pringle J. E., Begelman M. C., 1999, *MNRAS*, 310, 1002

- [34] Yuan F., Bu D. F., 2010, MNRAS, 408, 1051
- [35] Blandford R. D., Begelman M. C., 2004, MNRAS, 349,68
- [36] Xu G., Chen X., 1997, ApJ, 489, L29
- [37] Xue L., Wang J., 2005, ApJ,623, 372
- [38] Cowie L. L., Mckee C.F., 1977, ApJ, 275, 641
- [39] Xie F., Yuan F., 2012, MNRAS, arXiv:1207,3113
- [40] Johanson B. M., Quataert E., 2007,ApJ, 660, 1273
- [41] Meier D. L., 1979, ApJ, 233, 664
- [42] Meier D. L., 1982, ApJ, 256, 706